IJIE

UTHM Penerbit

INTERNATIONAL JOURNAL OF INTEGRATED ENGINEERING
ISSN: 2229-838X e-ISSN: 2600-7916

Vol. 18 No. 2 (2026) 68-81
https://publisher.uthm.edu.my/ojs/index.php/ijie

Coupled Reynolds–Mach–Thermal Dynamics in Vortex-Stabilized Meso-Scale Combustors: Implications for Efficiency and Stability

Azri Hariz Roslan[1,2], Mohd Al-Hafiz Mohd Nawi[2]*, Mohd Sharizan Md Sarip[3], Chu Yee Khor[2], Muhammad Lutfi Abd Latif[2], Mohammad Azrul Rizal Alias[2,4], Mohd Fathurrahman Kamarudin[2,5], Hazrin Jahidi Jaafar[2], Mohd Danish[6]

[1] *Kolej Vokasional Kangar, Jalan Sekolah Derma 01000 Kangar Perlis, MALAYSIA*
[2] *Faculty of Mechanical Engineering & Technology, Universiti Malaysia Perlis (UniMAP), Kampus Alam UniMAP, Pauh Putra, Arau, 02600, MALAYSIA*
[3] *Faculty of Chemical Engineering & Technology, Universiti Malaysia Perlis (UniMAP), 02600 Arau, Perlis, MALAYSIA*
[4] *Faculty of Ocean Engineering Technology, Universiti Malaysia Terengganu (UMT), 21030, Kuala Nerus, Terengganu, Malaysia, MALAYSIA*
[5] *Jabatan Kejuruteraan Mekanikal, Politeknik Tuanku Syed Sirajuddin (PTSS), 02600, Arau Perlis, MALAYSIA*
[6] *Department of Mechanical and Materials Engineering, University of Jeddah, Jeddah, 21589, SAUDI ARABIA*

*Corresponding Author: alhafiznawi@unimap.edu.my
DOI: https://doi.org/10.30880/ijie.2026.18.02.007

Article Info

Received: 25 August 2025
Accepted: 29 December 2025
Available online: 28 April 2026

Keywords

Meso-combustor, thermal, vortex flow, flame stabilization, central recirculation zones, CFD

Abstract

Meso-scale combustors have unique thermo-fluid challenges due to a high surface-to-volume ratio. Small changes in Reynolds number (Re) and Mach number (Ma) can have a big effect on how vortices behave, how heat moves, and how stable flames are. This study looks at how mass flow rate, Re, and Ma work together to change the temperature distribution in two vortex-stabilized combustor setups with different volumes. Current study works on high-fidelity CFD simulations using the RNG k–ε turbulence model with eddy dissipation chemistry over Re = 301.4–1153.8 (Ma<0.3), which stands for incompressible subsonic regimes. The results show that Re and Ma are directly proportional when the geometry and fluid properties stay the same. This makes it possible to predict how thermal fields will change with size. The larger-volume combustor always had stronger swirl and more coherent central recirculation zones (CRZs), which made the flame zones wider, improved radial heat transfer, and cut down on heat losses through the walls in all operating conditions. On the other hand, the compact combustor broke down vortices quickly, had steep radial temperature gradients, and was more likely to have flames put out at high Re. The results show a linked Re–Mach–temperature relationship that improves our ability to predict meso-scale combustion. This gives us a design framework to improve the stability, efficiency, and durability of portable power generation and micro-propulsion systems.

1. Introduction

The meso-scale combustor, typically characterized by diameters in the millimeter to centimeter range, presents a unique thermo-fluid environment where the interplay between Reynolds number (Re) and Mach number (Ma) critically governs flow structure, heat transfer, and combustion stability [1-2]. In such confined geometries, the elevated surface-to-volume ratio amplifies wall heat loss and renders the flame highly sensitive to variations in mass flow rate, inlet velocity, and residence time [3]. While the operating Re commonly spans from low to moderate ranges (≈ 300–1000), corresponding Mach number values generally remain within the subsonic regime (Ma < 0.3); nonetheless, even marginal variations in Mach number can influence the pressure–temperature field and alter flame anchoring behavior [4]. Previous investigations into meso-combustor configurations, including Tesla-valve structures [5] and swirl-inducing geometries [6-7], have demonstrated that increases in Re can enhance convective heat transfer and stabilize internal recirculation zones, yet may also diminish chemical efficiency due to reduced residence times [8]. High-fidelity computational studies employing Large Eddy Simulation (LES) and Direct Numerical Simulation (DNS) have further revealed combustion regime transitions, such as Flame Repetitive Extinction and Ignition (FREI) and Propagating Flame (PF) which are intrinsically linked to flow parameters and wall thermal conditions [9-10]. However, systematic quantification of temperature distribution, particularly along the combustor wall and at the exhaust plane, as a direct function of Re and Ma remains limited, with most prior works emphasizing flame dynamics or geometry optimization rather than fully coupled thermofluid behavior [11].

At higher mass-flow rates, increased Re and Ma intensify shear-layer turbulence in the CRZ, enhancing convective heat transport but reducing residence time, which can shift the peak temperature downstream and lower local flame temperatures for a fixed equivalence ratio. Higher Mach number also increases susceptibility to thermo-acoustic instabilities through stronger dynamic pressure fluctuations that couple with unsteady heat release. Conversely, at lower mass-flow rates, reduced Re and Ma extend the residence time and elevate peak temperatures, but at the cost of higher conductive heat loss to the walls and an increased risk of flashback if the laminar flame speed exceeds the local axial velocity. The stability and efficiency of vortex-stabilized meso-combustors therefore emerge from a delicate balance between vortex-induced mixing, acoustic feedback, and thermal energy retention. A clear understanding of these coupled Reynolds–Mach–Thermal dynamics is essential for optimizing mass-flow conditions that maximize combustion completeness while minimizing wall heat losses, mapping the blow-off and flashback limits in terms of non-dimensional groups, and establishing scaling laws that can be generalized to the design of next-generation meso-scale combustion systems. Such an approach aligns with the broader objective of enhancing both efficiency and stability in compact, high-power-density energy devices.

The primary impetus for studying small scale combustion systems arises from the wide array of possible applications they provide [12]. This section offers a succinct summary of many uses, including propulsion, actuation, power generation, and fuel reformation. From a combustion perspective, it is evident that when the system size reduces, there is a rise in heat losses and the probability of contact between the wall and radical species. These interactions can result in the suppression of the combustion event. In addition, when the system becomes smaller and shifts from turbulent to transitional flow, the effects of the boundary layer and friction, which are usually predictable and relatively unimportant compared to the system's energy output at larger sizes and high Reynolds numbers, can have a significant impact on the flow field's development [13-14]. The heat release rate is affected by both the Reynolds number and the equivalence ratio, as these factors are directly linked to the quantity of fuel burned [15]. The investigation of combustion within small-scale combustors has prompted the design of heat recirculation systems to address their increased flammability. Studies indicate that the design of small-scale combustors, along with the characteristics of their walls, significantly influences flame dynamics, flame structure, and flame location [6]. The Swiss-roll design was developed to enable the transfer of energy from combustion products to the unburned fuel–air mixture, thereby supporting the advancement of micro-power generation systems based on combustion [16-17]. According to [18], an increase in heat loss in a tiny Swiss-roll combustor (caused by using various combustor materials) leads to a reduction in the range of flammability of the combination. According to [19], raising the equivalence ratio or Reynolds number in a micro-scale Swiss-roll combustor shifts the reaction front from the centre of the combustor toward the inlet. This movement occurs because the reaction rate is enhanced [14] carried out an experiment using a small-scale Swiss-roll combustor, where heat recirculation from combustion gases to the unburned fuel–air mixture was applied to stabilize the flame. Their findings showed that the additional enthalpy from the recirculated burned gases raised the flame's peak temperature within the recirculation zone.

However, a quantitative coupling between Re and subsonic Ma that predicts wall and outlet temperature distributions in vortex-stabilized meso-combustors, especially under controlled volume scaling, remains insufficiently resolved in the literature. Here, we establish an explicit Re–Ma–temperature relationship and compare compact versus larger chambers under identical properties to derive design-relevant trends in stability and thermal efficiency. This study aims to investigate the influence of mass flow rate, Reynolds number (Re), and Mach number (Ma) on the temperature distribution and flame stabilization in vortex-stabilized meso-scale combustors of different chamber volumes. Moreover, its providing a foundation for optimizing meso-scale combustors with improved combustion efficiency, minimized wall heat loss, and enhanced operational stability, thereby contributing to the broader advancement of meso-scale combustion science and engineering applications.

This work establishes an explicit Reynolds–Mach–temperature linkage for vortex-stabilized meso-combustors, comparing compact vs larger volumes under identical thermophysical properties. By quantifying how Re and subsonic Ma co-vary with swirl persistence and CRZ strength, we show when mixing gains outweigh residence-time penalties, and we provide actionable design rules (volume scaling, target Re window, minimum swirl threshold) for portable power and micro-propulsion combustors.

2. Numerical Method

2.1 Governing Equations

The three-dimensional, steady-state Favre-averaged governing equations for mass, momentum, species mass fraction, and energy in Cartesian coordinates are applied in this study. These are given as follows:

$$\frac{\partial \rho \widetilde{u_j}}{\partial x_j} = 0 \tag{1}$$

$$\frac{\partial \rho \widetilde{u_i}\widetilde{u_j}}{\partial x_j} = -\frac{\partial P}{\partial x_i} + \frac{\partial}{\partial x_j}\left[(\mu + \mu_t)\left(\frac{\partial \widetilde{u_i}}{\partial x_j} + \frac{\partial \widetilde{u_j}}{\partial x_i}\right)\right] \tag{2}$$

$$\frac{\partial \rho \widetilde{u_j}\widetilde{Y_n}}{\partial x_j} = \frac{\partial}{\partial x_j}\left[(\rho D_n + \frac{\mu_t}{Sc_t})\frac{\partial \widetilde{Y_n}}{\partial x_j}\right] + \dot{\omega}_n \tag{3}$$

$$\frac{\partial \rho \widetilde{u_j}\widetilde{H}}{\partial x_j} = \frac{\partial}{\partial x_j}\left[\lambda \frac{\partial \tilde{T}}{\partial x_j} + \frac{\mu_t}{Pr_t}\frac{\partial \tilde{h}}{\partial x_j} + \sum_{n=1}^{N} \rho D_n h_n \frac{\partial \widetilde{Y_n}}{\partial x_j}\right] - \sum_{n=1}^{N} h_n^f \dot{\omega}_n \tag{4}$$

where ρ is the density, $u_{i/j}$ is the velocity vector components, P is the pressure, λ is the thermal conductivity, Pr_t is the turbulent Prandtl number, D_n is the mass diffusivity of species (n) which was assumed to be constant for each species, Y_n is the mass fraction of species (n), $\dot{\omega}_n$ is the chemical reaction rate, $\widetilde{H}$ is total enthalpy, μ is the dynamic viscosity and μ_t is the turbulent viscosity. The $\sim$ denotes the Favre averaging. Sc_t is the turbulence Schmidt number ($Sc_t = \mu_t/\rho D_t$ where D_t is a turbulence diffusivity). In the numerical procedure of this present study, various models of turbulence viscosity are examined.

2.2 Computational Approach

Using a second-order upwind scheme, the flow domain has been discretised using a three-dimensional (3D), finite volume solver. To make sure the solution is grid independent, several tetrahedral grids have been created. The mass conservation between the velocity terms and pressure in the discretised momentum equation has been obtained using the SIMPLE algorithm. The Eddy-Dissipation (ED) algorithm has been chosen for turbulence-chemistry interactions, and chemical reactions have been regarded as volumetric. The Arrhenius rate and chemical kinetics are disregarded in the ED reaction model, which solely makes use of the reaction flow parameters. The temperature and operating pressure were set at 300 K and 1.01 bars, respectively. The CFD code ANSYS Fluent was used to solve the governing equations using a steady state pressure-based solver. fluid in every simulation. With the exception of the energy equation and the chemical reactions equation, which converge at quantities less than 1×10−6, the solution is said to be converged when the residuals of each governing equation at successive iterations become less than 1×10−4. The flow field [20-21] variables reached stable local values under such circumstances, regardless of the number of iterations. Additionally, the temperature parameter monitors converged independently. Reacting flow cases were subjected to this convergence criterion. The specifics of the simulated asymmetric vortex flame's boundary condition are shown in Table 1. Figure 1 depicts the asymmetric vortex combustor's design, and the meso-scale combustor channel design is illustrated in Fig. 2, and the associated dimensions are listed in Table 2.

In order to assess the impact of grid sizes on the results, a grid independence test was implemented, as illustrated in Fig. 2. Figure 3 then consolidates the combustor geometry, boundary-condition placement, and domain meshing overview used for all reported simulations. The tetrahedral elements were employed to generate numerous mesh sets, and Scheme E was chosen with 113,133 nodes. The sensitivity study conducted indicates that the most suitable scheme should be implemented for all case studies and additions in order to minimize computing time. This test was conducted with laminar flow and a counter-flow configuration, with inlet air and inlet fuel (methane) temperatures set at 300 K. Scheme E, was determined to provide the optimal equilibrium between computational cost and accuracy among the evaluated schemes. The differences in key flow parameters between S_E and finer meshes (S_A and S_B) were negligible, with variations in core temperature and velocity magnitudes remaining below 1.5%. The comparative analysis against Khaleghi [22] indicates that Scheme E achieves the highest consistency with experimental data, exhibiting a MAPE of 2.07 % and a maximum deviation of 3.89 %, whereas Scheme C deviates substantially (MAPE ≈ 16.35 %). This confirms that Scheme E provides the most physically reliable numerical representation for the investigated flow regime. This level of agreement validates the numerical fidelity of S_E and confirms its suitability for use in all subsequent simulations. All computational domains included both fluid and solid regions of the meso-scale combustor. All computational tasks were executed on a workstation powered by an Intel Core i9 CPU and 16 GB of memory. Although the inlet Reynolds number based on D_h is in the 10^2– 10^3 range, the swirling jet and sudden expansion produce locally high shear and curvature; therefore, the flow is treated as transitional/turbulent and modelled using the RNG k–ε closure (swirl-dominated option) with second-order spatial discretization. This choice improves shear-layer mixing and CRZ persistence predictions compared with a laminar closure while remaining consistent with the subsonic regime (M<0.3).

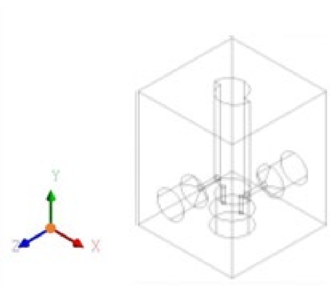

(a) Model Khaleghi (2015), D=1 mm

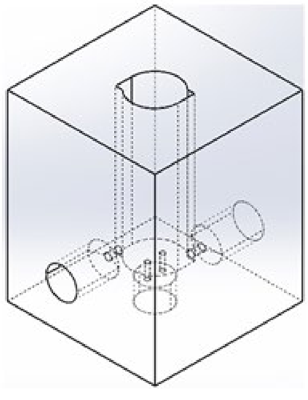

(b) Model A, D=1.5 mm

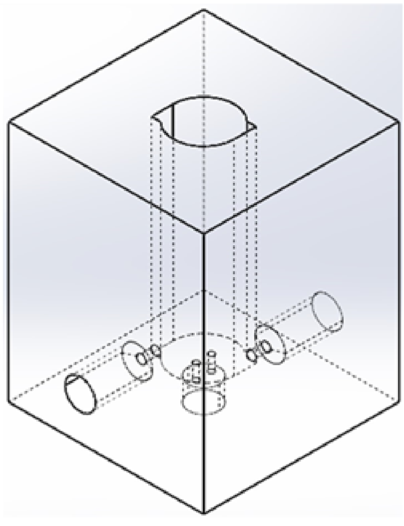

(c) Model B, D=2 mm

Fig. 1 *Vortex meso-scale combustor configurations; (a) Model Khaleghi (2015); d'$_{FI}$ = 1 mm; Model A; d'$_{FI}$ = 1.5 mm and (b) Model B; d'$_{FI}$ = 2.0 mm.*

Table 1 *Boundary condition settings (adapted from [22])*

Model	Settings	
Viscos model	RNG K-epsilon (2 Equations) RNG, with swirl-dominated flow option	
Radiation model	Discrete ordinate (DO)	
Reaction model	Model of turbulence chemistry with volumetric species transport reaction and eddy dissipation	
Boundary conditions	Air inlet	Mass flow rate: Various Temperature: 300 K Concentration: O_2 = 23%, N_2 = 77%
	Fuel inlet	Mass flow rate: Various

Table 2 *Geometric dimensions of meso-scale vortex combustors (mm)*

Samples	Model A	Model B
Length of meso chamber, L_{MC}	48	64
Height of meso chamber, H_{MC}	60	80
Diameter outlet, D_O	15	20
Diameter air inlet, D_{AI}	15	20
Diameter fuel inlet, D_{FI}	15	20
Diameter air inlet, d'_{AI}	2.25	3.0
Diameter fuel inlet, d'_{FI}	1.5	2.0
Length fuel inlet 1, H_{FI}, 1	7.5	10
Height-chamber, H_C	45	60
Volume	1.21x10-5 m^3	2.58x10-5 m^3

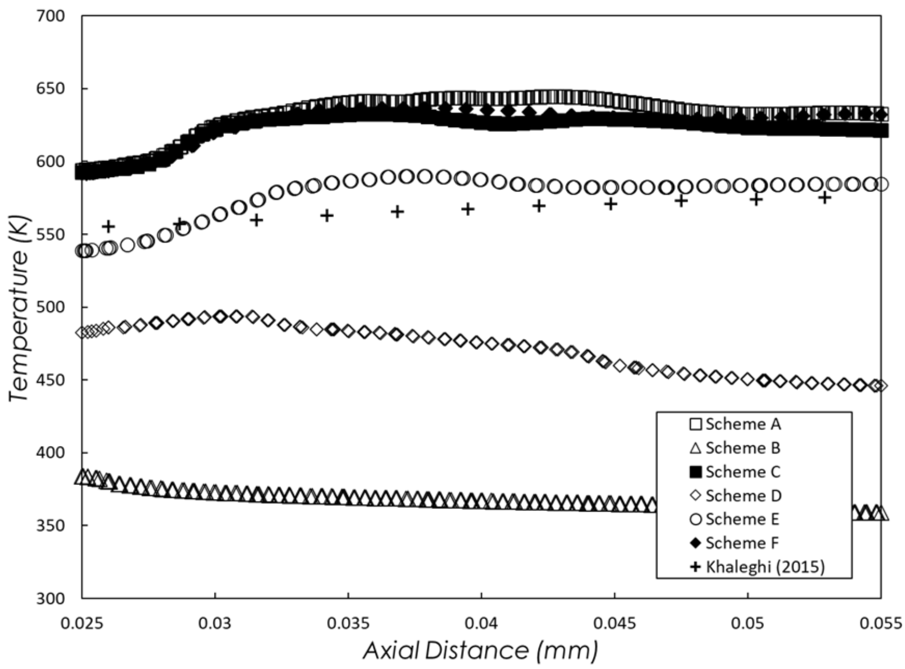

Fig. 2 *Vortex meso-scale combustor meshing schemes with scheme E selected*

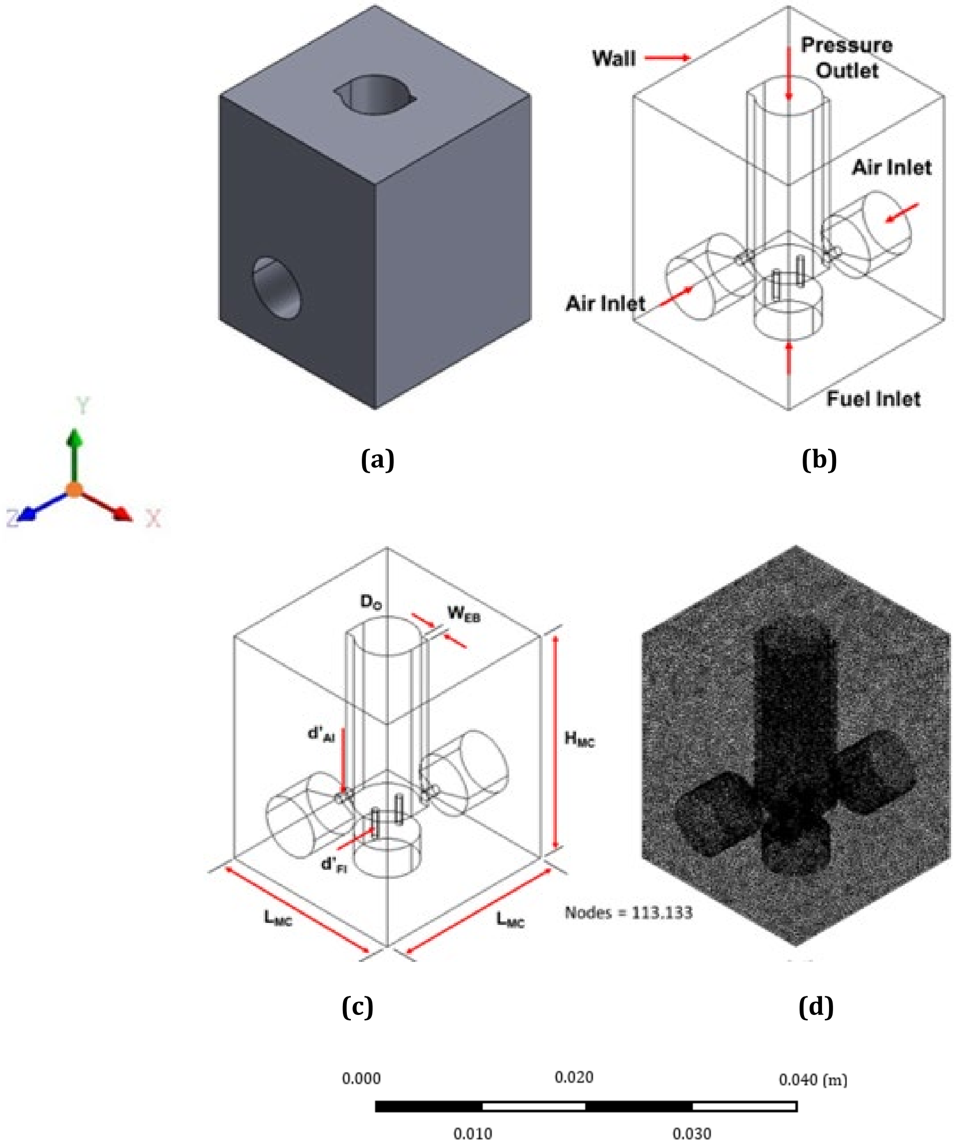

Fig. 3. *Description of meso-scale vortex combustor; (a) Isometric view; (b) Boundary conditions; (c) Dimensions and (d) Meshing*

3. Results and Discussion

3.1 Vortex Structure Characterization in Meso-Scale Combustors with Varying Volume Configurations

Figure 4 illustrates the three-dimensional vortex structures captured via iso-surface visualization techniques for two distinct meso-combustor volume configurations under varying flow conditions. The upper row represents a compact combustor geometry, while the bottom row corresponds to a higher volume design. A critical comparison reveals significant differences in swirling strength and vortex sustainability. In the lower volume combustor, vortex cores exhibit early dissipation and breakdown, characterized by irregular, fragmented structures and shorter axial penetration. This indicates suboptimal swirl number [23] or excessive wall-induced damping, leading to rapid decay of coherent vortex structures. Consequently, the early collapse of the vortex reduces fuel–air mixing efficiency and shortens the residence time [24], potentially compromising flame stabilization and increasing wall heat losses.

In contrast, the larger volume combustor demonstrates more elongated, coherent, and symmetrical vortex formations, extending further downstream along the combustion chamber. The pronounced swirling motion effectively generates a stronger internal recirculation zone, which improves thermal insulation by redirecting hot

Int. Journal of Integrated Engineering Vol. 18 No. 2 (2026) p. 68-81

products toward the combustor core and away from the walls. This promotes a more uniform temperature distribution and enhanced flame stabilization, especially under higher mass flow rates. The sustained vortex activity suggests an optimized swirl intensity that balances centrifugal forces and axial momentum. These observations underline the critical role of geometric scaling and swirl dynamics in governing the fluid behavior within meso-scale combustion systems. Properly tuning the combustor volume and swirl parameters [25] can significantly mitigate thermal losses while enhancing combustion efficiency in micro-energy applications [26].

3.2 Correlation Between Vortex Dynamics and Thermal Distribution in Meso-Scale Combustors

The axial temperature contours for both the compact-volume (left column) and large-volume (right column) meso-scale combustors across varying mass flow rates as in Fig. 4. The differences in flame structure and heat distribution are strongly governed by the interplay between vortex strength, recirculation characteristics, and combustor volume. In the compact combustor configuration, the flame core is narrow, with steep thermal gradients near the combustor wall. This behavior can be attributed to the early breakdown of the central vortex, resulting in diminished swirling strength and a weakened recirculation zone. The insufficient radial transport of high-temperature gases limits mixing between the fresh reactants and hot combustion products. Consequently, the residence time of the reacting flow is shortened, leading to incomplete combustion at higher flow rates. The heat energy remains concentrated along the core axis, which increases local heat flux toward the wall, intensifying thermal losses and elevating the risk of flame quenching. Such behavior is especially evident at higher mass flow rates where the velocity field dominates over the buoyancy-driven recirculation, further suppressing vortex stability.

In contrast, the large-volume combustor exhibits a more coherent and sustained vortex structure throughout the combustor length. The enhanced swirling strength facilitates stronger radial mixing, continuously transporting hot combustion gases toward the flame root region. This promotes a more uniform temperature rise along the axial direction and delays vortex breakdown to further downstream locations. The effect is a wider high-temperature core with gentler radial gradients, reducing the peak thermal load on the combustor walls and improving effective thermal insulation. The larger recirculation zones also act as thermal reservoirs, maintaining ignition stability across varying mass flow rates. From a fluid dynamics perspective, the correlation between swirling intensity and thermal field uniformity becomes more pronounced as combustor volume increases. Stronger swirl generates a larger central recirculation zone (CRZ), which enhances flame anchoring and stabilizes the combustion front. In the large-volume design, the CRZ remains intact over a broader range of Reynolds numbers, mitigating the adverse effects of velocity-induced vortex breakdown. By contrast, in the compact design, the CRZ collapses earlier, making the flame more sensitive to flow perturbations and mass flow rate variations. Thermally, the improved mixing induced by robust vortex motion in the large-volume combustor reduces localized hot spots and promotes a gradual radial decay of temperature. This not only enhances combustion efficiency but also reduces NO_x formation potential, as peak temperatures are moderated without compromising flame stability. The compact combustor, while potentially advantageous in minimizing size and material usage, sacrifices thermal uniformity and combustion completeness due to weaker swirl persistence.

Overall, these observations confirm that optimizing the swirling strength either through combustor geometry or inlet swirl generation plays a pivotal role in controlling both the vortex dynamics and the resultant temperature distribution. The large-volume combustor's superior ability to sustain strong and coherent vortex motion across different mass flow rates directly translates to higher combustion stability, improved thermal efficiency, and better tolerance to operational variations. This provides a compelling design direction for future high-performance meso-scale combustor systems aimed at portable power generation or micro-propulsion applications.

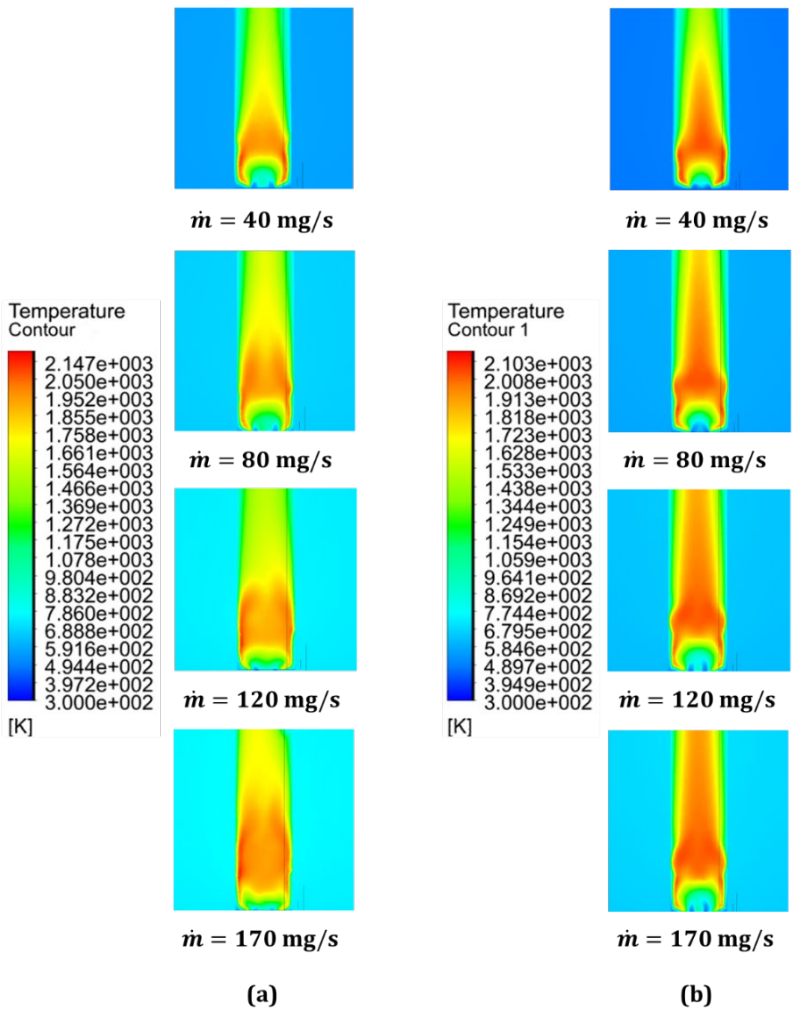

Fig. 4 *Temperature behaviour in meso-scale combustor; (a) model a; d'FI = 1.5 mm; (b) model b; d'FI = 2.0 mm*

3.3 Reynolds Number

The Reynolds number plays a key factor affecting flow behaviour within a vortex mixtures micro-scale combustor system orientated at a particular model of micro-scale combustor chamber and mass flow rate. Compared to the previous micro-scale combustor systems that consist of two inlet air jets and two inlet fuel jets with combustor diameter ranged from 10 mm and 14.4 mm in their study [22] conducted an extensive investigation of vortex flames. This study involved various micro-scale combustor chambers via a variety of equivalence ratio (φ) and mass flow rate (40 mg/s, 80 mg/s, 120 mg/s and 170 mg/s). As the flow enters the chamber, air jets positioned perpendicular to the fuel jets help to intensify the vortex flow within the micro-scale combustor. All types of micro-scale combustors share identical dimensions, except for the exhaust diameter. The flow was assumed to be non-slippery. To assess the impact of the Reynolds number, simulations were conducted at various mass flow rates of 40 mg/s, 80 mg/s, 120 mg/s and 170 mg/s respectively corresponding to 301.4, 577.6, 860.1 and 1153.8 Reynolds number, calculated from Equation (5 & 6).

$$Re = \frac{\rho V_I D_H}{\mu} \tag{5}$$

$$Re = \frac{4\dot{m}}{\pi D_H \mu} \tag{6}$$

In these calculations, the dynamic viscosity, μ, density of air, ρ, hydraulic diameter tube, $D_h = D$, velocity inlet, V_I, pi, π, and mass flow rate, $\dot{m}$, were all based on the specified inlet velocity conditions. Thus, this value indicates the presence of turbulent flow (Re > 4000) across all cases examined in this study. As illustrated in Fig. 5, Reynolds number results produced by the RNG $k - \varepsilon$ turbulence model closely align with those reported by previous researchers, [22]. The predicted axial temperature distribution at Re ≈ 301 shows close agreement with Kaleghi

[22], with a mean absolute percentage error (MAPE) of 2.5% and a maximum absolute deviation of 4.3% across the evaluated axial locations.

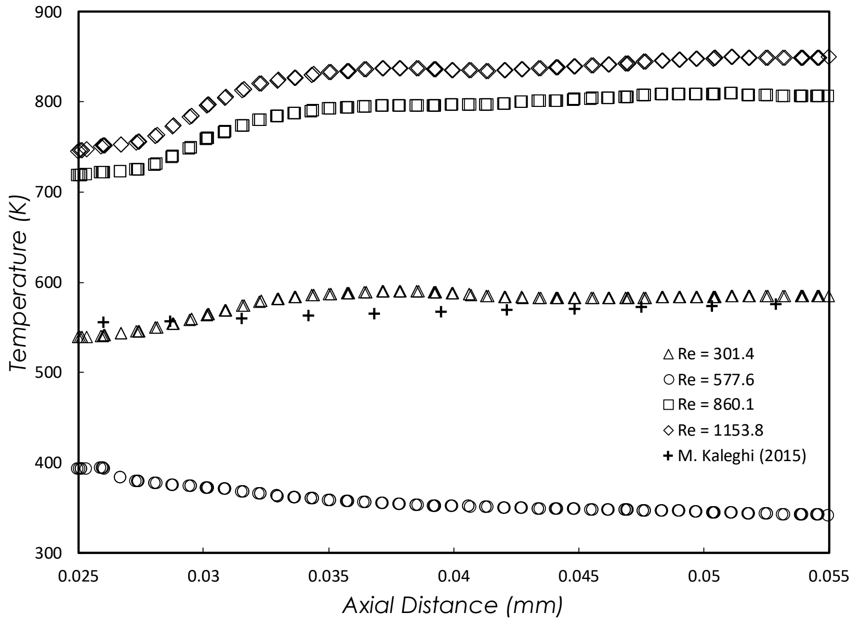

Fig. 5 *Temperature distribution at vortex mixtures micro-scale combustor for different Reynolds Numbers*

3.4 Mach Number

3.4.1 Influence of Reynolds Number on Mach Number and Temperature Distribution

The temperature distribution along the axial distance for Reynolds numbers $R_e = 301.4$, 577.6, 860.1, 1153.8 reveals a clear relationship between flow velocity, Mach number, and the thermal field development in the meso-combustor. At the lowest Reynolds number (Re = 301.4), the bulk velocity is relatively small, resulting in a Mach number well below the compressibility threshold (M<0.2), and the temperature profile remains moderate (~540–580 K) with minimal axial variation. As the Reynolds number increases to 577.6, the higher velocity leads to an increased Mach number, although still in the laminar regime. This promotes slightly enhanced convective heat transfer but also produces a small temperature drop near the inlet due to the stronger advective transport of cold reactants before significant combustion heat release occurs. For higher Reynolds numbers, particularly at Re=860.1 and 1153.8, the flow velocity and Mach number increase substantially. In laminar flows at meso-scale, the Mach number is directly proportional to Reynolds number when thermophysical properties remain constant, as both parameters scale linearly with velocity.

Although these higher Mach numbers remain in the subsonic regime (M<0.3), mild compressibility effects may begin to influence the structure of the thermal boundary layer. This behavior is reflected in the elevated downstream temperatures (~800 K for Re = 860.1 and ~850 K for Re = 1153.8), which indicate intensified convective mixing, more complete combustion, and greater heat release. These findings are consistent with previous studies [22] and recent micro-tube laminar flow analyses, which also reported a proportional Mach–Re relationship in subsonic regimes, followed by changes in behavior near transitional flow.

3.4.2 Mathematical Relationship between Mass Flow Rate, Reynolds Number, and Mach Number

In a steady laminar flow within a combustor of hydraulic diameter D_h the Reynolds number (Equation 1) is given where ρ is the fluid density, V is the mean axial velocity, and μ is the dynamic viscosity. The mass flow rate is expressed as:

$$\dot{m} = \rho A V \tag{7}$$

where A is the combustor cross-sectional area. From this, the velocity can be written as:

$$V = \frac{\dot{m}}{\rho A} \tag{8}$$

Substituting into the definition of Reynolds number:

$$R_e = \frac{\dot{m} D_h}{\mu A} \tag{9}$$

showing that for constant geometry and viscosity, R_e is directly proportional to $\dot{m}$. The Mach number is defined as:

$$M = \frac{V}{a} \tag{10}$$

where the local speed of sound is:

$$a = \sqrt{\gamma R T} \tag{11}$$

Substituting V from the mass flow equation:

$$M = \frac{\dot{m}/\rho A}{\sqrt{\gamma R T}} = \frac{\dot{m}}{\rho A \sqrt{\gamma R T}} \tag{12}$$

For an ideal gas where $\rho = {}^{p}/_{RT}$

$$M = \frac{\dot{m}\sqrt{\gamma R T}}{p A \sqrt{\gamma}} \tag{13}$$

Combining the above with the R_e expression gives:

$$M = \frac{\mu}{\rho D_h \sqrt{\gamma R T}} . R_e \tag{14}$$

This explicit relationship demonstrates that, for constant fluid properties and geometry, Mach number scales linearly with Reynolds number, and therefore with mass flow rate.

3.4.3 Numerical Estimation for Methane at 300 K, 100 kPa

Using methane properties at 300 K and 100 kPa as properties ($\gamma = 1.31, R = 518.3$ J/kg. K, $\mu = 1.10 \times 10^{-5}\ Pa.s, \rho \approx 0.643\ kg/m^3$), with a combustor hydraulic diameter $D_h = 0.01\ m$ and cross-sectional area $A = 7.854 \times 10^{-5} m^2$, the velocity and Mach number for each Reynolds number case are calculated as in Table 3. The Mach numbers for all tested Reynolds number cases are extremely small (M<0.3), confirming that the methane flow in the meso-combustor operates under incompressible laminar conditions. This indicates that density variations due to velocity are negligible, and the dominant mechanism influencing temperature distribution is convective heat transfer rather than compressibility. The proportional relationship between Reynolds number and Mach number highlights that increasing mass flow rate not only raises velocity but also enhances mixing and combustion efficiency, leading to higher downstream temperatures. This direct correlation provides a useful predictive tool when scaling combustor operation for different inlet conditions and strengthens the interpretation of the experimental temperature profiles presented in this study.

Table 3 *The correlation of Mach number and Reynolds number on preposition of flow regimes*

Case	R_e	$V\ (m/s)$	$Mach, M$	$\dot{m}\ (g/s)$	Flow Regime
1	301.4	0.515	0.00115	0.0259	Laminar, incompressible
2	577.6	0.986	0.00220	0.0501	Laminar, incompressible
3	860.1	1.468	0.00328	0.0741	Laminar, incompressible
4	1153.8	1.968	0.00440	0.0995	Laminar, incompressible

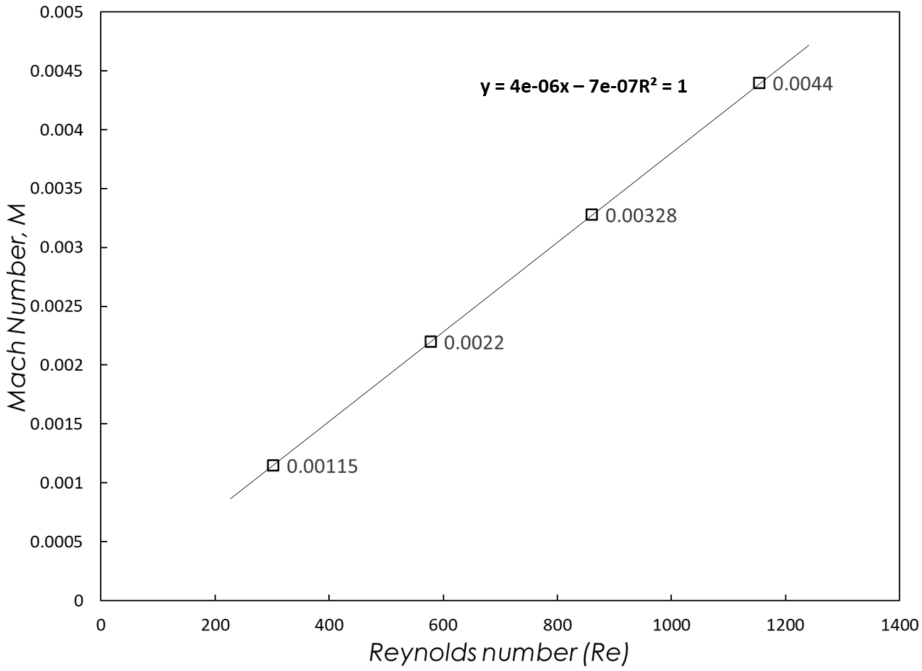

Fig. 6 *Relationship between Reynolds number and Mach number for Methane in Meso-Combustor*

3.4.4 Quantitative Analysis of Swirling Strength and Vorticity Magnitude

To complement the qualitative observations from Fig. 4, a quantitative assessment of the swirling strength and vorticity magnitude was conducted for both combustor configurations across the tested mass flow rates. Swirling strength λ_{ci} was evaluated based on the complex eigenvalues of the local velocity gradient tensor, enabling the identification of coherent vortex cores independently from shear-dominated regions. Vorticity magnitude (($|\vec{\omega}|$) was computed as:

$$|\vec{\omega}| = \sqrt{\left(\frac{\partial \omega}{\partial y} - \frac{\partial v}{\partial z}\right)^2 + \left(\frac{\partial u}{\partial z} - \frac{\partial w}{\partial x}\right)^2 + \left(\frac{\partial v}{\partial x} - \frac{\partial u}{\partial y}\right)^2} \quad (15)$$

where u, v, w are the velocity components in the x, y, z directions respectively.

(i) Compact-Volume Combustor

The peak swirling strength values were found close to the combustor inlet region, rapidly decaying downstream due to early vortex breakdown as shown in Fig. 4 Model A. This decay was more pronounced at higher mass flow rates, where increased axial momentum suppressed vortex coherence. The reduction in vorticity magnitude corresponded directly with the observed collapse of the central recirculation zone (CRZ), leading to weaker hot gas entrainment toward the flame base. The resulting temperature profile showed a steep axial gradient, with the peak temperature localized near the mid-length of the combustor.

(ii) Large-Volume Combustor
The larger-volume configuration demonstrated a more gradual decay in both swirling strength and vorticity magnitude, with coherent vortical structures persisting over a longer axial distance. At moderate mass flow rates, the swirl number (S) - calculated from the ratio of axial flux of angular momentum to axial flux of linear momentum, remained above the critical value of $S_{crit} \approx 0.6$, ensuring the maintenance of a strong CRZ. Even at higher mass flow rates, the swirl number stayed sufficiently high to delay vortex breakdown, thereby sustaining uniform heat release and enhancing overall combustion stability as shown in Fig. 4 Model B.

(iii) Thermal Implications
The correlation between swirling strength and temperature uniformity is evident - higher and sustained λ_{ci} values promote better radial mixing, distributing heat more evenly across the combustor cross-section. In the large-volume design (Refer to Fig. 1 and Fig. 4), the vorticity field creates a buffer region that shields the walls from peak flame temperatures, thereby reducing wall heat losses and extending combustor life. In contrast, the compact combustor's rapid loss of vortex coherence concentrates thermal energy in the core, increasing wall thermal stress and potentially accelerating material degradation.

(iv) Design Perspective
These findings highlight that for meso-scale combustors, the optimization of swirling strength through geometric tuning (swirl vane angle, inlet offset, or tangential entry) and volume scaling is as critical as fuel–air ratio control. For portable power generation or micro-propulsion applications, where operational stability across a wide range of flow conditions is essential, maintaining a swirl number above the critical threshold while ensuring sufficient combustor volume offers a robust pathway to achieving high combustion efficiency and thermal durability.

3.4.5 Design Implications

Design implications of coupled Re–Ma dynamics (Ma < 0.3). In the present meso-combustors, Mach number scales linearly with Reynolds number for fixed geometry and properties; thus, increases in $\dot{m}$ raise both Re and M while keeping the flow safely incompressible. Practically, this produces a trade-off: higher Re improves shear-layer mixing and strengthens CRZ-mediated heat recirculation, widening the high-T core; however, it also shortens residence time and can shift peak temperature downstream. Our results show that the larger-volume combustor sustains coherent swirl over a broader Re window, yielding more uniform temperature fields and lower wall heat fluxes; conversely, the compact volume suffers earlier vortex breakdown and steeper radial gradients at comparable Re. Accordingly, designers should (i) select a target Re band where mixing gains exceed residence-time penalties (in our cases, Re ≈ 600–1150), (ii) ensure swirl number ≥ ~0.6 to preserve a stable CRZ across the operating band, and (iii) use modest volume scaling (or outlet sizing) to delay breakdown and reduce wall losses without unduly increasing device footprint. Because M remains <0.3, compressibility effects are minor; however, incremental rises in M at the upper end of the Re range can enhance acoustic susceptibility, so baffling or damping features may be warranted in compact designs."

4. Conclusion

This work shows that, under stoichiometric conditions, temperature distribution and aerodynamic stability in meso-scale vortex combustors are co-governed by Reynolds number and geometry. Across Re ≈ 611–2341, higher Re strengthens the flame core and elevates peak temperatures. Model B (larger volume, wider inlets) consistently sustains broader, more symmetric high-temperature zones and a wider stability margin via improved mixing and longer residence time, whereas Model A (compact, smaller inlets) exhibits steeper near-wall gradients, greater asymmetry, and earlier instability at high Re. These findings motivate designs that ensure sufficient recirculation volume and balanced inlet momentum to minimize wall losses and maintain a uniform, high-temperature core.

Acknowledgement

The research has been carried out under the Fundamental Research Grant Scheme (FRGS)-Early Career (EC) (FRGSEC/1/2024/TK08/UNIMAP/02/31) provided by the Ministry of Higher Education.

Conflict of Interest

There is no conflict of interest regarding the publication of the paper.

Int. Journal of Integrated Engineering Vol. 18 No. 2 (2026) p. 68-81

Author Contribution

The authors confirm contribution to the paper as follows: ***study conception and design****: Muhammad Lutfi Abd Latif, Mohd Fathurrahman Kamarudin;* ***data collection****: Mohammad Azrul Rizal Alias;* ***analysis and interpretation of results****: Mohd Al-Hafiz Mohd Nawi, Mohammad Azrul Rizal Alias, Chu Yee Khor;* ***draft manuscript preparation****: Azri Hariz Roslan, Hazrin Jahidi Jaafar;* ***conceptualization****: Mohd Danish, Mohd Sharizan Md Sarip. All authors reviewed the results and approved the final version of the manuscript.*

References

[1] Sanata, A., Sholahuddin, I., Rosyadi, A. A., Nanlohy, H. Y., Nashrullah, M. D., Erawan, I. N. B., ... & Ramadhan, M. E. (2023). Characterization of biogas as an alternative fuel in micro-scale combustion technology. International Journal of Integrated Engineering, 15(4), 64-76. https://doi.org/10.30880/ijie.2023.15.04.006

[2] Sasongko, M. N., & Wijayanti, W. (2021). Experiment Investigation on the Effect of Oxygen Percentage on Combustion Characteristics of Waste Cooking Oil Biodiesel. International Journal of Integrated Engineering, 13(1), 39-45. https://doi.org/10.30880/ijie.2021.13.01.005

[3] Maruta, K. (2011). Micro and mesoscale combustion. Proceedings of the combustion institute, 33(1), 125-150. https://doi.org/10.1016/j.proci.2010.09.005

[4] Turns Stephen, R. (2000). An introduction to combustion: concepts and applications. Boston: McGraw-Hill, 158.

[5] Rong, H., & Zhao, D. (2025). Performance analyses on Telsa-valve structured meso-combustors in presence of ammonia-hydrogen/air combustion for thermophotovoltaic applications. Renewable Energy, 243, 122546. https://doi.org/10.1016/j.renene.2025.122546

[6] Minotti, A., & Sciubba, E. (2010). LES of a Meso Combustion Chamber with a Detailed Chemistry Model: Comparison between the Flamelet and EDC Models. Energies, 3(12), 1943-1959. https://doi.org/10.3390/en3121943

[7] Choi, M., Choi, K. W., Muhammad, H. A., & Lee, Y. D. (2024). Experimental investigation of combustion characteristics of a CH4/O2 premixed flame: Effect of swirl intensity on flame structure, flame stability, and emissions. Case Studies in Thermal Engineering, 55, 104069. https://doi.org/10.1016/j.csite.2024.104069

[8] Kuo, K. K., & Acharya, R. (2012). Fundamentals of turbulent and multiphase combustion. John Wiley & Sons.

[9] Aravind, A., Vadlamudi, G., & Basu, S. (2025). Dynamics of unsteady premixed flames in meso-scale channels and the effects of varying the wall heating conditions. Journal of Fluid Mechanics, 1008, A12. https://doi.org/10.1017/jfm.2025.113

[10] Chabane, A. M., Truffin, K., & Angelberger, C. (2020). Direct numerical simulation of catalytic combustion in a meso-scale channel with non-planar walls. Combustion and Flame, 222, 85-102. https://doi.org/10.1016/j.combustflame.2020.08.033

[11] Sheykhbaglou, S., Ghahremani, A., Tabejamaat, S., & Sánchez-Sanz, M. (2024). Comparative study of combustion and thermal performance of a meso-scale combustor under co-and counter-rotating fuel and oxidizer swirling flows for micro power generators. Heliyon, 10(2). https://doi.org/10.1016/j.heliyon.2024.e24250

[12] Deam, R. T., Lemma, E., Mace, B., & Collins, R. (2008). On scaling down turbines to millimeter size. Journal of Engineering for Gas Turbines and Power, 130(5), 1–9. https://doi.org/10.1115/1.2938516

[13] Fernandez-Pello, A. C. (2002). Micropower generation using combustion: Issues and approaches. Proceedings of the Combustion Institute, 29(1), 883–899. https://doi.org/10.1016/s1540-7489(02)80113-4

[14] Kim, N. Il, Aizumi, S., Yokomori, T., Kato, S., Fujimori, T., & Maruta, K. (2007). Development and scale effects of small Swiss-roll combustors. Proceedings of the Combustion Institute, 31 II, 3243–3250. https://doi.org/10.1016/j.proci.2006.08.077

[15] Cho, J. H., Lin, C. S., Richards, C. D., Richards, R. F., Ahn, J., & Ronney, P. D. (2009). Demonstration of an external combustion micro-heat engine. Proceedings of the Combustion Institute, 32 II(2), 3099–3105. https://doi.org/10.1016/j.proci.2008.07.017

[16] Fan, A., Zhang, H., & Wan, J. (2017). Numerical investigation on flame blow-off limit of a novel microscale Swiss-roll combustor with a bluff-body. Energy, 123, 252–259. https://doi.org/10.1016/j.energy.2017.02.003

[17] Samiran, N. A., Chong, C. T., Ng, J. H., Tran, M. V., Ong, H. C., Valera-Medina, A., Chong, W. W. F., & Mohd Jaafar, M. N. (2019). Experimental and numerical studies on the premixed syngas swirl flames in a model combustor. International Journal of Hydrogen Energy, 44(44), 24126–24139. https://doi.org/10.1016/j.ijhydene.2019.07.158

[18] Kim, N. Il, Kato, S., Kataoka, T., Yokomori, T., Maruyama, S., Fujimori, T., & Maruta, K. (2005). Flame stabilization and emission of small Swiss-roll combustors as heaters. Combustion and Flame, 141(3), 229–240. https://doi.org/10.1016/j.combustflame.2005.01.006

[19] Chen, M., & Buckmaster, J. (2004). Modelling of combustion and heat transfer in "Swiss roll" micro-scale combustors. Combustion Theory and Modelling, 8(4), 701–720. https://doi.org/10.1088/1364-7830/8/4/003

[20] Sharifzadeh, R., & Afshari, A. (2020). Numerical investigation of flow field effects on fuel–air mixing in a non-reacting trapped vortex combustor with different injection arrangements. European Journal of Mechanics-B/Fluids, 82, 106-122. https://doi.org/10.1016/j.euromechflu.2020.03.005

[21] Palies, P. (2025). Flow and Flame Mechanisms for Swirl-Stabilized Combustors. Aerospace, 12(5), 430. https://doi.org/10.3390/aerospace12050430

[22] Khaleghi, M., Hosseini, S. E., & Wahid, M. A. (2015). Vortex combustion and heat transfer in meso-scale with thermal recuperation. International Communications in Heat and Mass Transfer, 66, 250-258. https://doi.org/10.1016/j.icheatmasstransfer.2015.06.005

[23] Zhou, T., Zhao, K., Li, F., Wang, K., Meng, N., & Wang, D. (2023). Effects of swirl numbers on the unsteady characteristics of pilot flame in a triple-swirler staged combustor. Case Studies in Thermal Engineering, 44, 102846. https://doi.org/10.1016/j.csite.2023.102846

[24] Rowhani, A., Chinnici, A., Evans, M. J., Medwell, P. R., Nathan, G. J., & Dally, B. B. (2018). Variation of residence time in non-premixed turbulent bluff-body ethylene flames as a function of burner diameter. Proceedings of the 21st Australasian Fluid Mechanics Conference, AFMC 2018, December.

[25] Tang, C., Yao, Q., Jin, W., Li, J., Yan, Y., & Yuan, L. (2025). Effect of swirler geometry on the outlet temperature profile performance of a model gas turbine combustor. Applied Thermal Engineering, 260, 124946. https://doi.org/10.1016/j.applthermaleng.2024.124946

[26] Choi, J., Rajasegar, R., Lee, T., & Yoo, J. (2020). Development and characterization of swirl-stabilized diffusion mesoscale burner array. Applied Thermal Engineering, 175, 115373. https://doi.org/10.1016/j.applthermaleng.2020.115373